Gonadal Hormones And Frontocortical Expression Of Vascular Endothelial Growth Factor In Male Stroke- Prone, Spontaneously Hypertensive Rats, A Model For Attention-Deficit/Hyperactivity Disorder

Authors
Subrina Jesmin, Hiroko Togashi, Ichiro Sakuma, **Chishimba N. Mowa**, Ken-Ichi Ueno, Taku Yamaguchi, Mitsuhiro Yoshioka, And Akira Kitabatake

Abstract
Attention-deficit/hyperactivity disorder (AD/HD) is a common pediatric behavioral disorder associated, in part, with male preponderance and reduced regional cerebral blood flow (rCBF). However, mechanism(s) underlying male preponderance and reduced rCBF in AD/HD are unclear. The present study profiles the expression of angiogenic and hormonal factors likely to underlie these symptoms using a recently characterized AD/HD animal model, juvenile male stroke-prone spontaneously hypertensive rats (SHRSP). Because vascular endothelial growth factor (VEGF) signaling cascade and gonadal steroids are key regulators of angiogenesis and gender based behavior, respectively, we profiled their patterns of expression in the frontal cortex of SHRSP to elucidate their roles in the genesis of AD/HD male preponderance and rCBF. Interestingly, levels of VEGF, VEGF receptors (KDR, Flt-1), endothelial nitric oxide synthase, phosphorylated Akt (pAkt), estrogen receptor-B, aromatase, and capillary density in sham-operated SHRSP were remarkably down-regulated, whereas androgen receptor levels were up-regulated, compared with age-matched genetic control, Wistar-Kyoto rats. Castration, estrogen, and androgen receptor antagonist (flutamide) counteracted these effects. Dihydrotestosterone, but not testosterone, reversed the beneficiary effects of castration. Estrogen receptor-B levels remained unchanged in all groups examined. We postulate that changes in androgen metabolism that tend to up-regulate local dihydrotestosterone concentration and diminish estrogen synthesis, in the frontal cortex of juvenile male SHRSP, may lower levels and/or activity of VEGF and its signaling cascade and, subsequently, reduce rCBF. These findings could, in part, help explain the pathogenesis of reduced rCBF and male preponderance in AD/HD.

Subrina Jesmin, Hiroko Togashi, Ichiro Sakuma, **Chishimba N. Mowa**, Ken-Ichi Ueno, Taku Yamaguchi, Mitsuhiro Yoshioka, And Akira Kitabatake (2004) "Gonadal Hormones and Frontocortical Expression of Vascular Endothelial Growth Factor in Male Stroke-Prone, Spontaneously Hypertensive Rats, a Model or Attention-Deficit/Hyperactivity Disorder" *Endocrinology* 145(9): 4330-4343 Version of Record Available At www.academic.oup.com
[DOI: 10.1210/en.2004-0487]

ATTENTION-DEFICIT/HYPERACTIVITY DISORDER (AD/HD) is a common pediatric behavioral disorder characterized by inattention, hyperactivity, and impulsivity that can lead to social, affective, and learning impairments at school (1, 2). Because boys are 6–9 times more prone to be diagnosed with AD/HD (3, 4) and because volumetric abnormalities in regional cerebral blood flow (rCBF) in some brain regions, including the frontal cortex and striatum, are common in AD/HD (2, 5–11), key factors likely to play important roles in AD/HD pathogenesis include gender- and vascular-associated factors.

The precise factors that underlie male preponderance in AD/HD have not been fully elucidated. The possible involvement of gonadal hormones in AD/HD male preponderance is based on their critical role in shaping developmentally programmed sex differences in the forebrain (12, 13) and their involvement in several psychopathologies (14). Importantly, a growing body of evidence indicates involvement of gonadal hormones and their receptors in the pathogenesis and clinical symptom manifestations in AD/HD subjects, although conclusive mechanistic insights and explanations are yet to be clarified (15–20). Gonadal hormones influence key projecting neurons, including dopaminergic and cholinergic systems that play a major role in rCBF and whose regulation is disrupted in AD/HD (3, 15, 16, 21–33). Indeed, dopaminergic or cholinergic interventions restore rCBF and cerebral dysfunction in AD/HD patients (23, 34) and animal models (35, 36). Alternatively, gonadal hormones are, in addition, likely to directly influence rCBF by modulating factors that regulate vascular development and function, such as vascular endothelial growth factor (VEGF) (37–40). VEGF is widely distributed in multiple cell types of the central nervous system (CNS) and is known to exert a trophic effect on endothelial, neuronal, and glial cells, an essential process during CNS development and repair (41). VEGF optimal concentration in the CNS is critical and, for this reason, tightly regulated to maintain optimal activity (42). Intermediate or suboptimal VEGF levels lead to decreased blood vessel branching and density in the cerebral

---

Abbreviations: AD/HD, Attention-deficit/hyperactivity disorder; AR, androgen receptor; aromatase, aromatase P450; CNS, central nervous system; DHT, dihydrotestosterone; E, 17*β*-estradiol; eNOS, endothelial NO synthase; ER, estrogen receptor; ERKO, ER knockout; GSA-B4, *Griffonia simplicifolia*; NO, nitric oxide; pAkt, phosphorylated Akt; PVDF, polyvinylidene diflouride filter; rCBF, regional cerebral blood flow; SHR, spontaneously hypertensive rat; SHRSP, stroke-prone SHR; TPBS, PBS containing 0.1% Tween 20; Ts, testosterone; VEGF, vascular endothelial growth factor; WKY, Wistar-Kyoto rat.

cortex (42), and severe reductions of VEGF are fatal, leading to hypoxia and, subsequently, degeneration of cerebral cortex and neonatal lethality (42). Collectively, these observations strongly support the hypothesis that alterations of VEGF concentration orchestrated by changes in gonadal hormone synthesis and/or metabolism, at a critical time of frontal cortex development, could compromise rCBF. These changes may predispose the animal to AD/HD.

Several animals have been proposed as models of AD/HD (43–45). However, very few sufficiently exhibit the symptomatic and therapeutic profiles seen in AD/HD patients. For instance, in the most commonly used model, spontaneously hypertensive rats (SHRs), male preponderance is not observed, whereas female, but not male, SHRs exhibit impulsivity-inattention, although both are hyperactive (46). Furthermore, the effectiveness of psychostimulants in SHRs is not consistent with the behavioral paradigms used (47). We recently established juvenile stroke-prone SHRs (SHRSPs), a substrain of SHR, as a new animal model for AD/HD (35, 36). Interestingly, this animal model, apparently, exhibits all the key behavioral symptoms seen in human AD/HD subjects, including hyperactive, impulsive-like behavior, and/or inattention (35). Furthermore, similar to human AD/HD subjects, SHRSPs exerted male preponderant impairment in attentional performance, which was normalized by clinical dosages of methylphenidate (35). Neurochemical and cognitive studies of male SHRSPs revealed dopaminergic hypofunction in the prefrontal cortex, nucleus accumbens shell, striatum, and basolateral amygdala (48) as well as cognitive impairment, accompanied by central cholinergic dysfunction (49). Moreover, the SHRSP displays higher motor activity than the SHR (50), and cerebrospinal fluid serotonin levels are significantly decreased in the SHRSP, but not in the SHR, as compared with genetic control Wistar-Kyoto rats (WKYs) (51).

More recently, we found that gonadal hormone manipulations altered the behavior of juvenile male SHRSPs (52). Male SHRSPs exhibited an impairment in spontaneous alternation performance in a Y-maze, compared with the genetic control, WKYs, which was ameliorated by gonadectomy (castration for 21 d) (52) but counteracted by replacement of the nonaromatizable androgen, dihydrotestosterone (DHT) (for 3 wk at 250 μg/kg, daily) (52). Surprisingly, the aromatizable androgen, testosterone (300 μg/kg, daily), antiandrogen (flutamide) (10 mg/kg, daily, 21 d) or 17β-estradiol (E; 10 μg/kg, daily, 21 d), unlike DHT, did not reverse the effects of gonadectomy on spontaneous alternation performance in SHRSPs (52). These findings suggest that alterations in gonadal hormone levels or metabolism may be one of the factors that underlie short-term memory deficit in male juvenile SHRSPs, an animal model of AD/HD (52).

Thus, in the present study, we used juvenile (6 wk old) male SHRSPs to elucidate factors likely to underlie male preponderance and volumetric abnormalities in the frontal cortex of SHRSPs by examining the expression profiles of: 1) VEGF and basic VEGF signaling machinery [VEGF receptors (KDR and Flt-1), phosphorylated Akt (pAkt), and endothelial nitric oxide (NO) synthase (eNOS)]; 2) plasma gonadal steroid hormones [estrogen, testosterone (Ts), DHT]; 3) gonadal steroid hormone receptors [estrogen receptor (ER), androgen receptor (AR)]; and 4) aromatase P450 (aromatase). Furthermore, the effects of castration and exogenous gonadal steroid hormones on the expression of the above molecules in SHRSP were investigated.

Materials and Methods

Animal Models

Juvenile male SHRSPs (6 wk of age), inbred in our laboratory (current generation, F57), and a gender- and age-matched genetic control, WKYs (n = 20), were used in this study. All animals were kept under standard laboratory conditions (temperature of 22 ± 2 C and 12-h light, 12-h dark cycle). Forty SHRSPs, castrated at 3 wk of age, were divided into three groups treated sc (dorsally, on the neck) daily for 21 d with: 1) 10% ethanol in sesame oil (vehicle) (5 ml/kg, n = 14); 2) Ts (300 μg/kg, n = 14); or 3) DHT (250 μg/kg, n = 12). In addition, 44 sham-operated 3-wk-old SHRSPs were divided into three groups treated daily for 21 d with: 1) 10% ethanol in sesame oil, vehicle (5 ml/kg, n = 20), 2) E (10 μg/kg, n = 12); or 3) flutamide, an AR blocker (10 mg/kg, n = 12) administered sc (dorsally, on the neck). Four to six hours after the last injection, animals were anesthetized with ketamine chloride (50 mg/kg, ip) (decapitation was not done), blood samples were collected via abdominal aortic puncture, and then brain tissues were harvested and either snap frozen in liquid nitrogen and preserved at -80 C (for cryostat sections, Western blot analysis or real-time PCR) or postfixed in 4% paraformaldehyde overnight (for paraffin sections). In another set of experiments, WKYs, which served as genetic control for SHRSPs, were also castrated (n = 6) at 3 wk of age and then killed after 3 wk for tissue harvest, as described above. All experimental procedures were approved and performed in accordance with Hokkaido University School of Medicine Animal Care and Use Committee.

Determination of plasma levels of E, Ts, and DHT

Plasma levels of E, Ts, and DHT were determined by enzyme immunoassay using the following kits: 1) rodent estradiol ELISA test kit (Endocrine Technologies, Inc., Newark, CA), 2) estradiol EIA kit (Cayman Chemical, Ann Arbor, MI), 3) Ts ELISA (Immuno-Biological Laboratories, Hamburg, Germany), 4) Ts EIA kit (Cayman Chemical), 5) rodent Ts ELISA test kit (Endocrine Technologies), and 6) DHT ELISA (Immuno-Biological Laboratories).

Comparable results were found for E and Ts from the kits mentioned above. The data presented in this manuscript for E and Ts were obtained using the kits of rodent estradiol ELISA test kit (Endocrine Technologies) and Ts ELISA (Immuno-Biological Laboratories), respectively.

Immunolabeling

Immunolabeling studies were undertaken to determine the expression patterns of VEGF, Flt-1, KDR, eNOS, ERα, ERβ, AR, and aromatase expression in the frontal cortex of SHRSPs and WKYs. The specificities of these antibodies have been well characterized in our previous reports (53–57).

Eight 10-μm-thick frozen coronal cryostat (VEGF, Flt-1, KDR, eNOS, aromatase) and 5-μm-thick paraffin (AR, ERα and -β, aromatase) sections of frontal cortex cut serially were immunolabeled as previously described (53–57). The paraffin sections were deparaffinized and treated for 20 min with citrate buffer [10 mm citric acid (pH 6.0)] in a microwave oven (750 W) before immunostaining. To prevent nonspecific staining, the cryostat and paraffin sections were blocked with nonimmune serum (1% BSA in Tris). The sections were then incubated overnight at 4 C with primary antibodies, rinsed in phosphate buffer solution and then exposed to the fluorescence secondary antibody, Cy3-conjugated AffiniPure goat antirabbit IgG or fluorescein-conjugated AffiniPure goat antirabbit, antigoat and antimouse IgG (Jackson ImmunoResearch Laboratories, West Grove, PA), for 2 h, according to the manufacturer's instructions. Sections processed without primary antibodies served as negative controls. The coverslips were mounted with Immunon (Thermo Shandon, Pittsburgh, PA). Immunofluorescent images were viewed using the laser scanning confocal imaging system (model MRC-1024; Bio-Rad Laboratories, Maryland, UK). The following antibodies,

which are commercially available, were used: rabbit antihuman VEGF polyclonal antibody (Immunological Laboratories, Fujioka, Japan), rabbit antihuman KDR polyclonal antibody (Santa Cruz Biotechnology, Santa Cruz, CA), rabbit antihuman Flt-1 polyclonal antibody (Santa Cruz Biotechnology), rabbit antihuman eNOS polyclonal antibody (Affinity BioReagents, Golden, CO), mouse ERα monoclonal antibody (Novocastra Laboratories, Newcastle upon Tyne, UK), rabbit antihuman ERβ polyclonal antibody (Affinity BioReagents), rabbit antihuman AR polyclonal antibody (Chemicon International, Temecula, CA), and rabbit antihuman aromatase polyclonal antibody (Santa Cruz Biotechnology).

Western blot analysis

After removing and rinsing the frontocortical tissues in sterilized PBS on ice, the tissues were minced with scissors, homogenized, and centrifuged at 500 X *g* for 15 min to pellet any insoluble material. The protein concentration of supernatant was determined using the bicinchoninic acid protein assay (Pierce, Rockford, IL). Samples were run on SDS-PAGE, using 7.5–15% polyacrylamide gel, and electrotransferred to polyvinylidene diflouride filter (PVDF) membrane. To reduce nonspecific binding, the PVDF membrane was blocked for 2 h at room temperature with 5% nonfat milk in PBS containing 0.1% Tween 20 (TPBS). Thereafter, the PVDF membrane was incubated overnight at 4 C with specific antibodies for VEGF, KDR, Flt-1, eNOS, pAkt (Ser 473) antibody (Cell Signaling Technology, Beverly, MA), ERα, ERβ, AR, and aromatase in TPBS; washed thrice in TPBS; and then (PVDF) incubated with horseradish peroxidase-conjugated antirabbit (Amersham, Buckinghamshire, UK), antimouse (Amersham), or antigoat antibody (Santa Cruz Biotechnology) diluted at 1:2,000–10,000 in TPBS at room temperature for 60 min. The blots were visualized with the enhanced chemiluminescence detection system (Amersham), exposed to x-ray film, and analyzed using free NIH image software.

Immunoassay of VEGF and pAkt

VEGF levels in rat frontocortical tissue (n = 8/group) were measured using a commercially available kit (VEGF immunoassay, R&D Systems, Minneapolis, MN), according to the manufacturer's instructions.

The level of Akt protein, phosphorylated at serine residue 473, in frontocortical tissue extract was quantitatively determined by ELISA kit, Akt (pS473) (BioSource International, Inc., Camarillo, CA).

NO colorimetric assay

NO was indirectly detected in brain tissue extracts as nitrite using a nitric oxide colorimetric assay kit (Roche Diagnostics GmbH, Mannheim, Germany). In this method, the nitrate present in the sample was reduced to nitrite by reduced nicotinamide adenine dinucleotide phosphate in the presence of the enzyme nitrate reductase. The nitrite formed reacted with sulfanilamide and *N*-(1-naphthyl)-ethylenediamine dihydrochloride to give a red-violet diazo dye. The diazo dye was measured at 550 nm, on the basis of its absorbance within the visible range.

In situ hybridization

Twenty-micrometer-thick serial frozen coronal sections of frontal cortex were prepared and mounted on glass slides precoated with 3-aminopropyltriethoxysilane. The sections were then fixed by 4% paraformaldehyde with 0.25% acetic anhydride in 0.1 m triethanolamine-HCl (pH 8.0). The hybridization procedure was performed as previously described (53–58). The specificities of the probes used in the present investigation have already been well characterized in our previous reports (53–58). The probes were complementary to nucleotide residues 61–106 of VEGF cDNA (accession no. AF239170), 541–585 of KDR cDNA (accession no. U93306), 961-1016 of Flt-1 cDNA (accession no. D28498), 841–885 of eNOS cDNA (accession no. X76309), 301–346 of ERα cDNA (accession no. Y00102), 45–90 of ERβ cDNA (accession no. U57439), and 1621–1666 of AR cDNA (accession no. NM012502). Specific 60-bp-long oligonucleotides of the rat cytochrome P450 aromatase cDNA used by Lauber and Lichtensteiger (59) were purchased. The oligonucleotides were labeled with ^{35}S-dATP using terminal deoxyribonucleotidyl transferase. The radiolabeled probes were hybridized to the tissue in a prehybridization buffer for 10 h at 42 C. The sections were either exposed to Hyperfilm-βmax (Amersham) for 4 wk or dipped in NTB2 nuclear track emulsion (Kodak, Rochester, NY) and exposed for 4–8 wk. The specificity of *in situ* hybridization was confirmed by the disappearance of signals when excess doses of the corresponding nonlabeled (^{35}S-dATP) antisense oligonucleotides (cold) were added to the labeled antisense oligonucleotides (hot) hybridization fluid. Consistent mRNA signals for each molecule above background levels were considered positive and were scored, subjectively, as strong, moderate, or weak.

RNA preparation and real-time quantitative PCR

Protocol used for the real-time quantitative PCR in the present study has already been published in a previous report (56). Total RNA samples were prepared from frontocortical tissues by the guanidinium thiocyanate-phenol-chloroform single-step extraction method with Isogen (Nippon Gene, Toyama, Japan) used routinely in our laboratory (56). After being isolated, treated with DNase I, and quantified, RNA was reverse transcribed to cDNA by the use of a ReverTra Ace (Toyobo, Osaka, Japan).

The single-stranded cDNA was then used in real-time quantitative PCR for evaluation of relative expression levels of the eight genes of interest. Selected genes and primers are shown in Table 1. DNA amplification was performed in the Applied Biosystems (ABI 7900HT) real-time PCR machine with the GeneAmp 7900HT sequence detection system software (PerkinElmer Corp., Foster City, CA), and the detection was made by measuring the binding of the fluorescence dye SYBR Green I to double-stranded DNA. The PCRs were set up in microtubes in a volume of 20 μl. The reaction components were 2 μl cDNA synthesized as above, 10 μl of 2X SYBR Green master mix (PerkinElmer Corp.), and 0.4 μm of each pair of oligonucleotide primers (Table 1). The program was as follows: an initial step at 95 C for 10 min and then 40 cycles of 95 C for 15 sec and 60 C for 60 sec. Regression curves were drawn for each sample, and its relative amount was calculated from the threshold cycles with the instrument's software (SDS 2.0) according to the manufacturer's instructions. The PCR products were analyzed by gel electrophoresis to confirm the specificity of generated products. Relative expression levels of the target genes were normalized to the geometric mean of the two internal control genes, β-actin and glyceraldehyde-3-phosphate dehydrogenase.

Capillary morphology

Previous studies have shown that histochemical staining with the lectin *Griffonia simplicifolia* (GSA-B4) is a sensitive and reliable method

TABLE 1. Primers and conditions for real-time quantitative PCR analyses

Gene	Primers (5'–3')		Product size (bp)
	Sense	Antisense	
VEGF	GTACCTCCACCATGCCAAGT	GCATTAGGGGCACACAGGAC	194
KDR	CAGAAAAGGAGATGCCCGAC	TCCAGAGTTTTCAGCTCTTC	300
Flt-1	AGGAGAGGACCTGGAACTGTCTT	ATTCCTGGGCTCTGCAGGCATAG	470
eNOS	CTGCTGCCCCAGATATCTTC	CAGGTACTGCAGTCCCTCCT	230
ERα	CTTCTGGAGTGTGCCTGGTT	CTTCTCCCTGCAGGTTCATC	199
ERβ	CCTTGAAGGCTCTCGTGTTA	TAGAAGACGCCATCCAAAGG	200
AR	CAACTTGCATGTGGATGACC	TGAGAAAGGTGCCTCATCCT	198
Aromatase	CCTGGAGATGACGTGATTG	CGATGTACTTCCCAGCACAG	197

to visualize the capillary vasculature in the frontal cortex of rat brain (53). Eight-micrometer-thick serial frozen coronal sections of frontal cortex were stained with GSA-B4 (Sigma Chemical, St. Louis, MO). The sections were fixed with acetone, air dried, and placed in PBS. After being treated with 3% H_2O_2 in methanol and washed in PBS, the sections were incubated with GSA-B4 (1:100 dilution in PBS) overnight at 4 C, followed by reaction with streptoavidin conjugated to peroxidase (Nichirei Corp., Tokyo, Japan) and through rinse in PBS. For visualization diaminobenzidine/H_2O_2 as chromogen was used. To enhance the diaminobenzidine reaction, the sections were rinsed with 0.05 m $NaHCO_3$ (pH 9.6) and then incubated in diaminobenzidine enhancing solution (Vector Laboratories, Burlingame, CA). Vascular endothelium was stained with lectin, which stained capillaries as black/dark brown dots. Sections were examined using a microscope (Olympus, Tokyo, Japan), and counts were made of stained capillaries in cross-sections in 30 fields (117,617 μm^2/field) per sample (section on slide) at a final magnification of X400 by an image-analyzing software (microcomputer imaging device, Imaging Research, St. Catharine, Ontario, Canada). This counting method has been well established by previous reports (53, 54, 57). Furthermore, the number of lectin-stained capillaries were quantified by two independent researchers in a double-blinded study. Care was taken to avoid counting the same single capillary twice. Any microvessel (defined as a vessel having internal diameter < 100 μm) that had no apparent lumen was considered as a single capillary.

Capillary density was also assessed light-microscopically on 5-μm-thick deparaffinized tissue sections that were immunostained by anti-von Willebrand factor (FVIII) antibody (53) (Dako, Hamburg, Germany) or CD34 (Santa Cruz Biotechnology). The antibodies were made visible by a secondary exposure of the sections to Cy3-conjugated AffiniPure donkey antirabbit IgG (Jackson ImmunoResearch Laboratories).

Statistical analysis

Data are expressed as the mean ± sd. Homogeneity of variance between groups was checked by Bartlett's test. Data were compared using one-way ANOVA (ELISA data, basal data of immunoblot, capillary density). *Post hoc* comparisons were made with Scheffé's multicomparison test. A two-tailed Student's *t* test was used to analyze differences between two group means (sham-operated WKY and castrated WKY). Differences were considered significant at $P < 0.05$.

Results

Plasma levels of Ts, DHT, and E

Plasma levels of Ts (1.52 ± 1.30 ng/ml, n = 12) and DHT (0.24 ± 0.10 ng/ml, n = 12) in sham-operated SHRSPs were significantly ($P < 0.01$) higher than those of WKYs (Ts: 0.73 ± 0.45 ng/ml, n = 12; DHT: 0.13 ± 0.07 ng/ml, n = 12). After castration, levels of Ts and DHT were markedly decreased in SHRSPs: Ts (0.20 ± 0.18 ng/ml, n = 10) and DHT (0.03 ± 0.01 ng/ml, n = 10) ($P < 0.01$).

Replacement with Ts (300 μg/kg·d) for 21 d restored plasma levels of Ts in castrated SHRSPs (1.44 ± 0.78 ng/ml, n = 10) identical to that in sham-operated SHRSPs. DHT plasma levels decreased to 0.10 ± 0.05 ng/ml (n = 10) after Ts replacement in castrated SHRSPs, compared with sham-operated SHRSPs.

Replacement with DHT (250 μg/kg·d) for 21 d restored plasma levels of DHT (0.22 ± 0.10 ng/ml) in castrated SHRSPs to those observed in sham-operated SHRSPs. However, plasma Ts levels remained unchanged after DHT replacement in castrated SHRSPs (0.3 ± 0.01 ng/ml), compared with vehicle-treated castrated SHRSPs.

Treatment of sham-operated SHRSPs with E (10 μg/kg·d), on the contrary, markedly decreased ($P < 0.01$) plasma levels of both Ts (0.24 ± 0.05 ng/ml) (n = 10) and DHT [below detectable levels (<0.02 ng/ml, n = 10)], compared with sham-operated SHRSPs.

Treatment of sham-operated SHRSPs with AR blocker, flutamide (10 mg/kg·d), also significantly ($P < 0.01$) decreased plasma Ts (0.30 ± 0.29 ng/ml, n = 10) and DHT levels (0.09 ± 0.07 ng/ml, n = 10), compared with sham-operated SHRSPs.

Plasma levels of E (12.01 ± 5.37 pg/ml, n = 16) were significantly ($P < 0.01$) lower in sham-operated SHRSPs than WKYs (22.45 ± 6.67 pg/ml, n = 16) and decreased further after the castration of SHRSPs (6.01 ± 4.03 pg/ml, n = 6) ($P < 0.01$). Administration of E significantly increased plasma levels of E (70.02 ± 50.1 pg/ml, n = 8; $P < 0.001$) in sham-operated SHRSPs. Furthermore, Ts replacement in castrated SHRSPs changed plasma E levels to 25.0 ± 11.2 pg/ml (n = 8), which was almost comparable with those in WKYs.

Expression of VEGF and receptors (KDR, Flt-1)

Strong immunofluorescent staining for VEGF and its receptors (KDR and Flt-1) were localized in the microvessels of the frontal cortex from WKYs (Fig. 1). In contrast, in sham-operated SHRSPs, they were weakly stained but increased

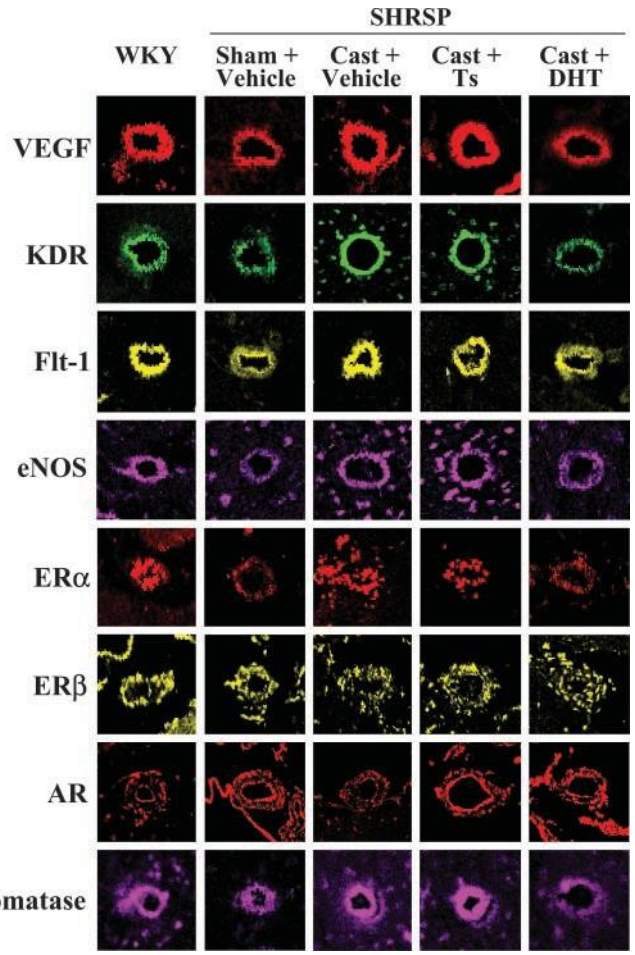

FIG. 1. Frontocortical serial sections from genetic control WKYs and SHRSPs [sham-operated (sham+vehicle), castrated SHRSPs (cast+vehicle), castrated SHRSPs replaced with Ts (cast+Ts), and castrated SHRSPs replaced with DHT (cast+DHT)] immunostained for VEGF, KDR, Flt-1, eNOS, ERα, ERβ, AR, and aromatase. Positive staining was shown in cerebral microvessels (internal diameter < 100 μm) of the frontal cortex. Magnification, X200.

after castration in SHRSPs (Fig. 1). Although Ts replacement had no effect on the levels of VEGF, KDR, and Flt-1 in castrated SHRSPs, DHT replacement down-regulated the castration-induced expression of VEGF, KDR, and Flt-1 (Fig. 1). Using Western blot analysis, VEGF, KDR, and Flt-1 proteins in the rat frontocortical tissues extracts were detected as single bands migrating at 39, 200, and 180 kDa, respectively (Figs. 2, A and B, and 3A). Densitometric analysis for these bands revealed a significant ($P < 0.001$) reduction in relative protein levels of the frontocortical tissues from sham-operated SHRSPs, compared with those of WKYs (Figs. 2, A and B, and 3A). Consistent with immunohistochemical data, VEGF, KDR, and Flt-1 protein levels were significantly increased after castration of SHRSPs, attenuated by DHT replacement (Figs. 2, A and B, and 3A). Ts replacement exerted no effect on expression of these molecules in castrated SHRSPs (Figs. 2, A and B, and 3A). When sham-operated SHRSPs were treated with E or flutamide, levels of VEGF, KDR, and Flt-1 were up-regulated (Figs. 2, A and B, and 3A). Frontocortical levels of VEGF, as determined by ELISA, showed a

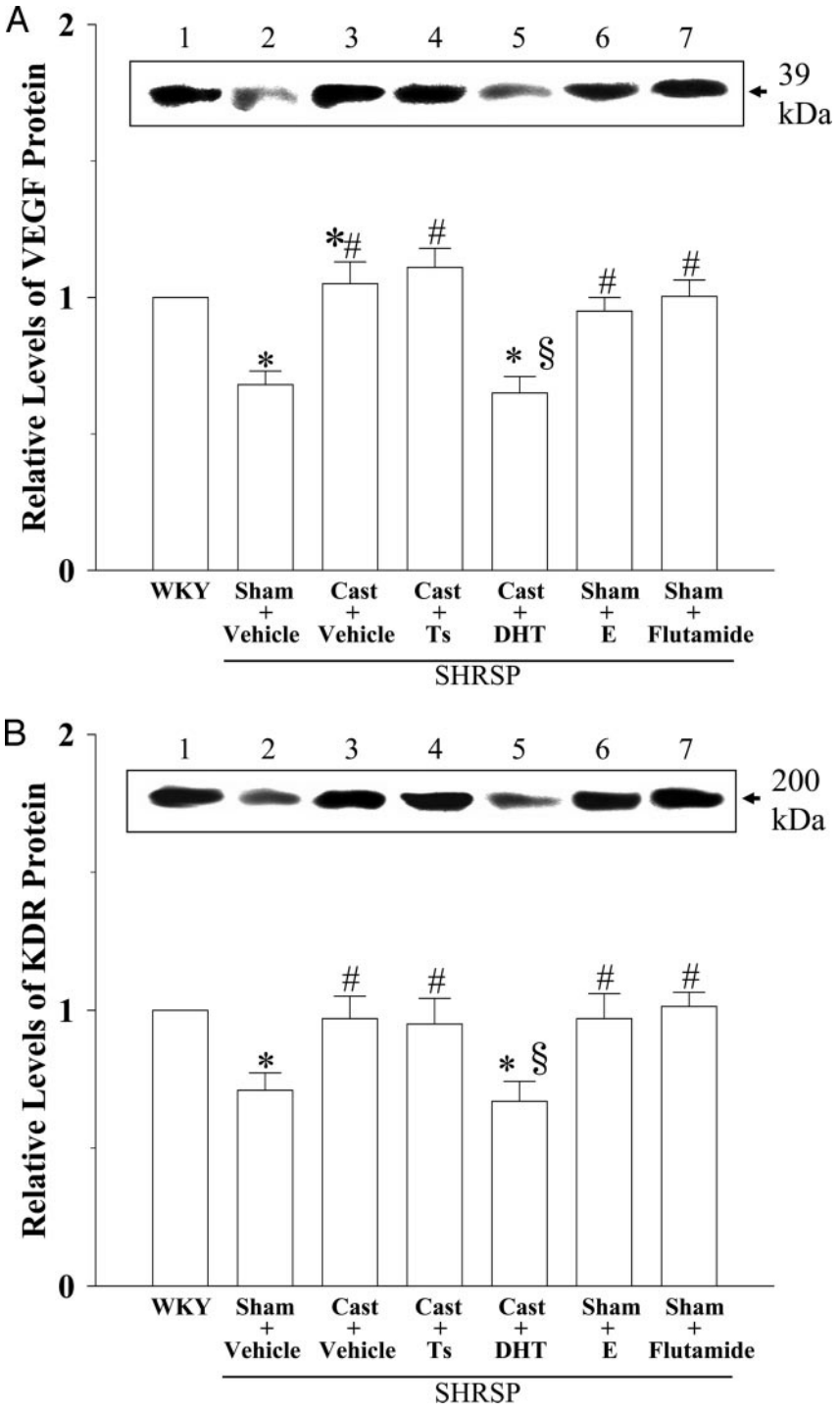

FIG. 2. A and B, Immunoblot analysis for VEGF (A), and KDR (B) in the frontocortical tissues of genetic control WKYs (lane 1), sham-operated SHRSPs (sham+vehicle) (lane 2), castrated SHRSPs [vehicle treated (cast+vehicle) (lane 3); Ts replaced (cast+Ts) (lane 4); DHT replaced (cast+DHT) (lane 5)], sham-operated SHRSPs treated with E (sham+E) (lane 6), and sham-operated SHRSPs treated with flutamide (sham+flutamide) (lane 7). The *panel of bands*, just above the histogram, shows representative blots of the type of animal and/or treatment, as described above. The intensity of the bands were plotted as histograms, as shown below each panel. In each of the experiments, the band obtained with control WKYs is normalized as 1.0. Data are shown as means ± SD of five separate experiments. Statistical analysis was done for the basal data before normalization using one-way ANOVA followed by Scheffé's multicomparison test. *, $P < 0.001$ *vs.* WKY; #, $P < 0.001$ *vs.* sham-operated SHRSP; §, $P < 0.001$ *vs.* castrated SHRSP (vehicle).

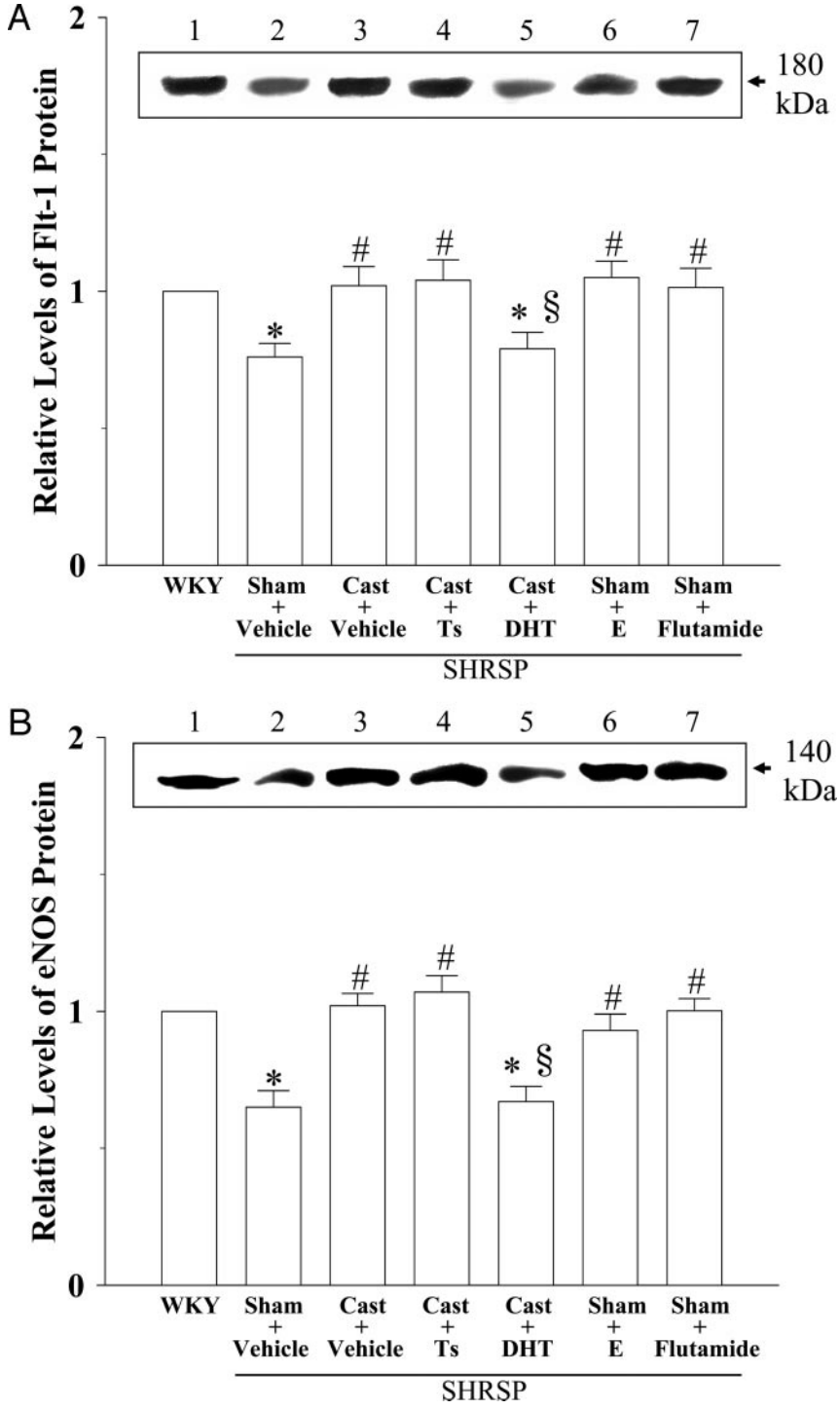

FIG. 3. A and B, Immunoblot analysis for Flt-1 (A) and eNOS (B) in the frontocortical tissues of genetic control WKYs (lane 1), sham-operated SHRSPs (sham+vehicle) (lane 2), castrated SHRSPs [vehicle treated (cast+vehicle) (lane 3); Ts replaced (cast+Ts) (lane 4); DHT replaced (cast+DHT) (lane 5)], sham-operated SHRSPs treated with E (sham+E) (lane 6), and sham-operated SHRSPs treated with flutamide (sham+flutamide) (lane 7). The *panel of bands*, just above the histogram, shows representative blots of the type of animal and/or treatment, as described above. The intensity of the bands were plotted as histograms, as shown below each panel. In each of the experiments, the band obtained with control WKYs is normalized as 1.0. Data are shown as means ± SD of five to seven separate experiments. Statistical analysis was done for the raw data before normalization using one-way ANOVA followed by Scheffé's multicomparison test. *, $P < 0.001$ *vs.* WKY; #, $P < 0.001$ *vs.* sham-operated SHRSP; §, $P < 0.001$ *vs.* castrated SHRSP (vehicle).

significant ($P < 0.01$) decrease in sham-operated SHRSPs (16 ± 4 pg/mg), compared with WKYs (22 ± 3 pg/mg). However, after castration VEGF levels in SHRSPs were increased to 23 ± 4 pg/ml. Ts replacement maintained the increased VEGF levels in castrated SHRSPs (25 ± 4 pg/mg). DHT replacement in castrated SHRSPs decreased VEGF levels (13 ± 3 pg/mg) nearly to those observed in sham-operated SHRSPs.

Interestingly, contrary to the effects on SHRSPs, castration of WKYs resulted in a small (15 ± 6%) but significant ($P = 0.006$) decrease in VEGF levels in the frontal cortex, compared with sham-operated WKYs, as revealed by ELISA.

In situ hybridization (see Fig. 7) and real-time PCR (Table 2) data corresponded to those of immunohistochemistry and Western blot analysis described earlier: VEGF, KDR, and Flt-1 mRNA signals were: 1) reduced in the frontocortical tissues of sham-operated SHRSPs, compared with those in WKYs, and up-regulated after E or flutamide treatment; and

TABLE 2. Relative amounts of mRNAs in the frontal cortex in different groups compared with values in WKY control rats

Genes	WKY	SHRSP					
		Sham+vehicle	Cast+vehicle	Cast+Ts	Cast+DHT	Sham+E	Sham+flutamide
VEGF	1	0.74	1.10	1.20	0.77	1.05	1.11
KDR	1	0.75	1.16	1.13	0.78	0.98	1.12
Flt-1	1	0.78	1.13	1.21	0.80	0.97	1.14
eNOS	1	0.77	0.95	1.03	0.65	0.96	1.02
ER-*a*	1	0.61	1.20	1.50	0.71	1.15	1.19
ER-*β*	1	1.02	1.00	0.95	0.97	1.01	0.99
AR	1	1.35	0.85	1.32	1.36	0.94	1.20
Aromatase	1	0.79	1.00	1.35	0.78	1.15	1.21

Total RNA was extracted from the frontal cortex and subjected to real-time PCR quantification, as described in *Materials and Methods*. Values represent the amount of mRNA relative to that in WKY control rats, which is arbitrarily defined as 1. Sham-operated SHRSP (sham+vehicle), castrated SHRSP [vehicle treated- (cast+vehicle); testosterone replaced- (cast+Ts); dihydrotestosterone replaced- (cast+DHT)], sham-operated SHRSP treated with estrogen (sham+E), and sham-operated SHRSP treated with flutamide (sham+flutamide).

2) increased after castration of SHRSPs and down-regulated after DHT replacement in castrated SHRSPs.

Expression of eNOS

Both the distribution and expression patterns of eNOS mRNA and protein in the frontal cortex of sham-operated SHRSPs (vehicle, E, or flutamide), castrated SHRSPs (vehicle, Ts, or DHT), and genetic control WKYs matched those of VEGF above (Figs. 1, 3B, and 7; and Table 2). The predicted size of eNOS bands (~140 kDa) were detected in frontocortical tissues (Fig. 3B).

Levels of NO (as nitrite)

Frontocortical nitrite levels in sham-operated SHRSPs and control WKYs were 3.0 ± 0.5 and 4.2 ± 0.2 nmol/mg ($P <$ 0.01), respectively. Ts replacement in castrated SHRSPs raised the nitrite level to 5.1 ± 0.4 nmol/mg, but DHT replacement strongly lowered the nitrite level in castrated SHRSPs to 2.7 ± 0.3 nmol/mg. E and flutamide treatments in sham-operated SHRSPs increased nitrite levels also to 4.7 ± 0.4 and 4.4 ± 0.4 nmol/mg, respectively.

Expression of pAkt

Reduction of VEGF levels described above is expected to impact the expression of signaling molecule downstream of VEGF. Because Akt is an important downstream signaling molecule in VEGF-induced angiogenesis, we sought to determine whether there are changes in its expression in sham-operated SHRSPs and WKYs, as seen in VEGF. pAkt was clearly visualized as a major band with a molecular mass of 55 kDa in rat frontocortical tissues using immunoblot analysis (Fig. 4A). However, levels of pAkt in the frontal cortex of: 1) sham-operated SHRSPs treated with vehicle, E, or flutamide; 2) castrated SHRSP treated with vehicle, Ts, or DHT; and 3) WKYs matched those of VEGF, described above, using Western blot analysis (Fig. 4A) and ELISA (Fig. 4B), indicating a disruption of VEGF signaling.

Expression of ERα, ERβ, and aromatase

To determine whether the estrogen-ER system is disrupted in sham-operated SHRSPs, we investigated the expression patterns of ERα, ERβ, and aromatase, the enzyme that converts Ts to estrogen.

ERα, ERβ. ERβ, the major subtype expressed in the frontocortical neurons, remained unchanged in both sham-operated SHRSPs and WKYs, in all groups examined (see Figs. 1, 5B, and 7; and Table 2), whereas ERα expression showed a pronounced change, which was strikingly similar to that of VEGF described earlier, based on immunohistochemical (Fig. 1), Western blot analysis (Fig. 5A), *in situ* hybridization (Fig. 7), and real-time PCR data (Table 2). ER bands of predicted size (ERα, 65 kDa; ERβ, 55 kDa) were detected in the frontocortical tissues using NCL-ER-6F11 (ERα) and PA1–311 (ERβ) antisera (Fig. 5, A and B). The specificities of these antibodies in rat tissues have been well characterized in our previous report (55) by using controls, including omission of the primary antiserum, omission of the secondary antibody, and adsorption of the primary antiserum with its respective antigen. These procedures were also repeated in the brain tissue in the present study (data not shown).

Aromatase. The expression of cytochrome P450 aromatase protein (Figs. 1 and 6B) and mRNA (Fig. 7 and Table 2) matched that of ERα, described earlier. The down-regulated aromatase was attenuated by castration of SHRSPs and, subsequently, reverted to precastration levels by replacement with DHT but not Ts (Figs. 1, 6B, and 7; and Table 2). The predicted size of aromatase bands (~58 kDa) was detected in the frontal cortex (Fig. 6B).

Expression of AR

The increase in plasma levels of Ts and DHT in sham SHRSPs led us to examine the frontocortical pattern of their receptor, AR. Corresponding to the pattern of its ligands, Ts and DHT, AR expression levels in sham-operated SHRSPs were up-regulated but down-regulated after castration (Figs. 1, 6A, and 7; and Table 2). Administration of both ligands to castrated SHRSPs significantly increased ($P <$ 0.01) AR levels (Figs. 1, 6A, and 7; and Table 2). In contrast, E treatment in sham-operated SHRSPs significantly down-regulated AR ($P <$ 0.01) (Fig. 6A and Table 2), whereas flutamide treatment only slightly down-regulated AR expression ($P <$ 0.05) (Fig. 6A and Table 2). The predicted size of AR bands (~98 kDa) was detected in the frontal cortex (Fig. 6A).

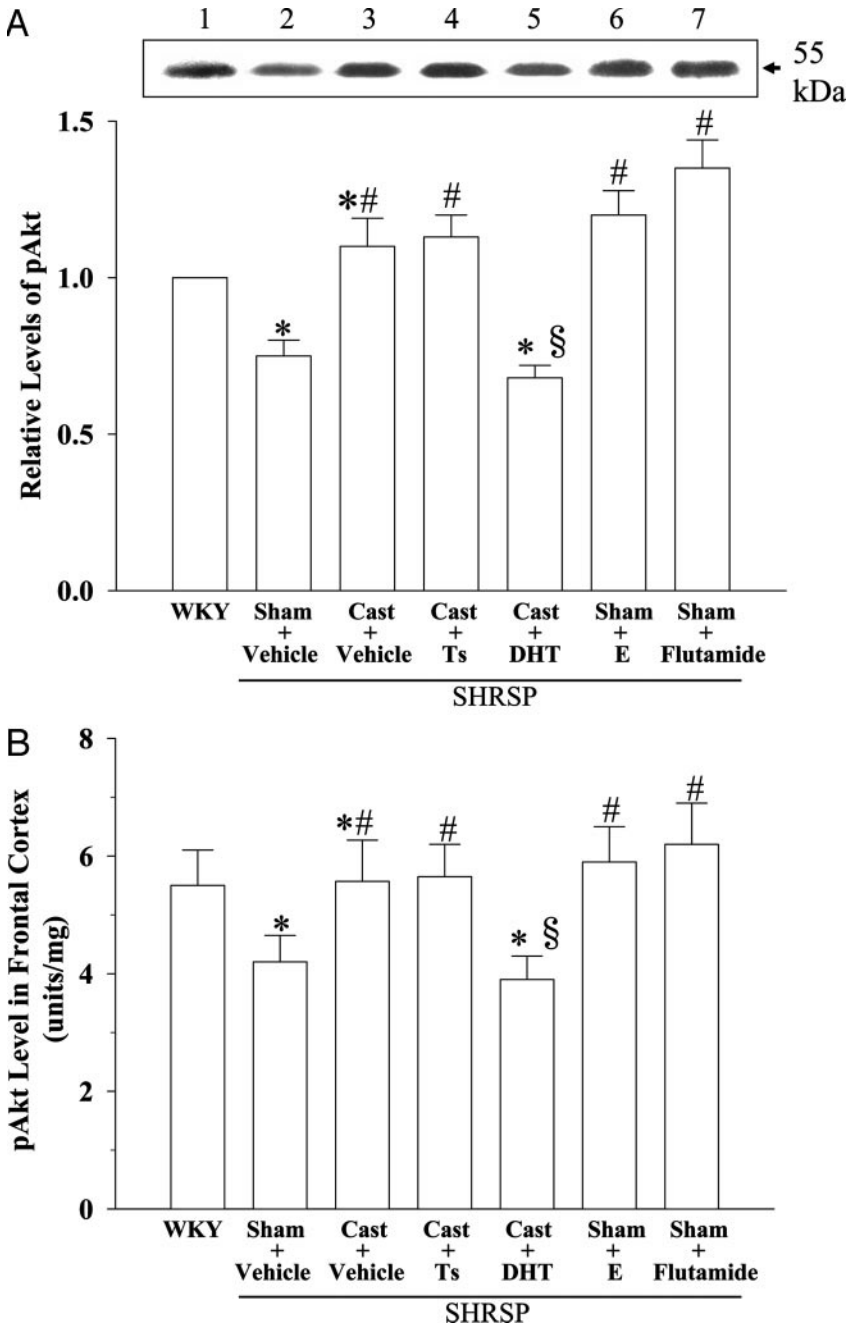

FIG. 4. A and B, Immunoblot analysis for pAkt (A) in the frontocortical tissues of genetic control WKYs (lane 1), sham-operated SHRSPs (sham+vehicle) (lane 2), castrated SHRSPs [vehicle treated (cast+vehicle) (lane 3); Ts replaced (cast+Ts) (lane 4); DHT replaced (cast+DHT) (lane 5)], sham-operated SHRSPs treated with E (sham+E) (lane 6), and sham-operated SHRSPs treated with flutamide (sham+flutamide) (lane 7). The *panel of bands*, just above the histogram, shows representative blots of the type of animal and/or treatment, as described above. The intensity of the bands were plotted as histograms, as shown below the panel (A). In each of the experiments, the band obtained with control WKYs is normalized as 1.0. Data are shown as means ± SD of five separate experiments. B, The level of Akt protein that is phosphorylated at serine residue 473 in frontocortical tissue extract (n = 8) was quantitatively determined by ELISA. Data are shown as means ± SD. For both immunoblot and ELISA, statistical analysis was done using one-way ANOVA followed by Scheffé's multicomparison test. *, $P < 0.001$ *vs.* WKY; #, $P < 0.001$ *vs.* sham-operated SHRSP; §, $P < 0.001$ *vs.* castrated SHRSP (vehicle).

Capillary morphology

Capillary density in the frontal cortex of sham-operated SHRSPs, as determined by GS4 lectin staining, was significantly lower (29%), compared with genetic control WKYs. However, this trend was reversed by castration of SHRSP rats, resulting in a remarkable increase in GS4 lectin-stained capillaries in frontal cortex that was almost comparable with WKYs (Fig. 8) (capillary density: WKY, sham SHRSP, castrated SHRSP, 980 ± 120, 686 ± 100, 965 ± 105/mm^2). Fluorescent immunostaining for FVIII and CD34 (data not shown) yielded comparable results to GS4 lectin.

Discussion

Our study used a new animal model for AD/HD, juvenile male SHRSPs, and began to investigate angiogenic (VEGF signaling machinery) and hormonal factors likely to underlie two common phenomenons, namely reduced rCBF and male preponderance, associated with AD/HD (5–11). Plasma levels of DHT and Ts in sham-operated SHRSPs increased about 2-fold, compared with WKYs, the genetic control animal. In contrast, levels of VEGF signaling cascade [VEGF, VEGF receptors (KDR and Flt-1), pAkt, and eNOS], ER*a*, aromatase, and capillary density were significantly down-regulated in the frontal cortex of sham-operated SHRSPs, com-

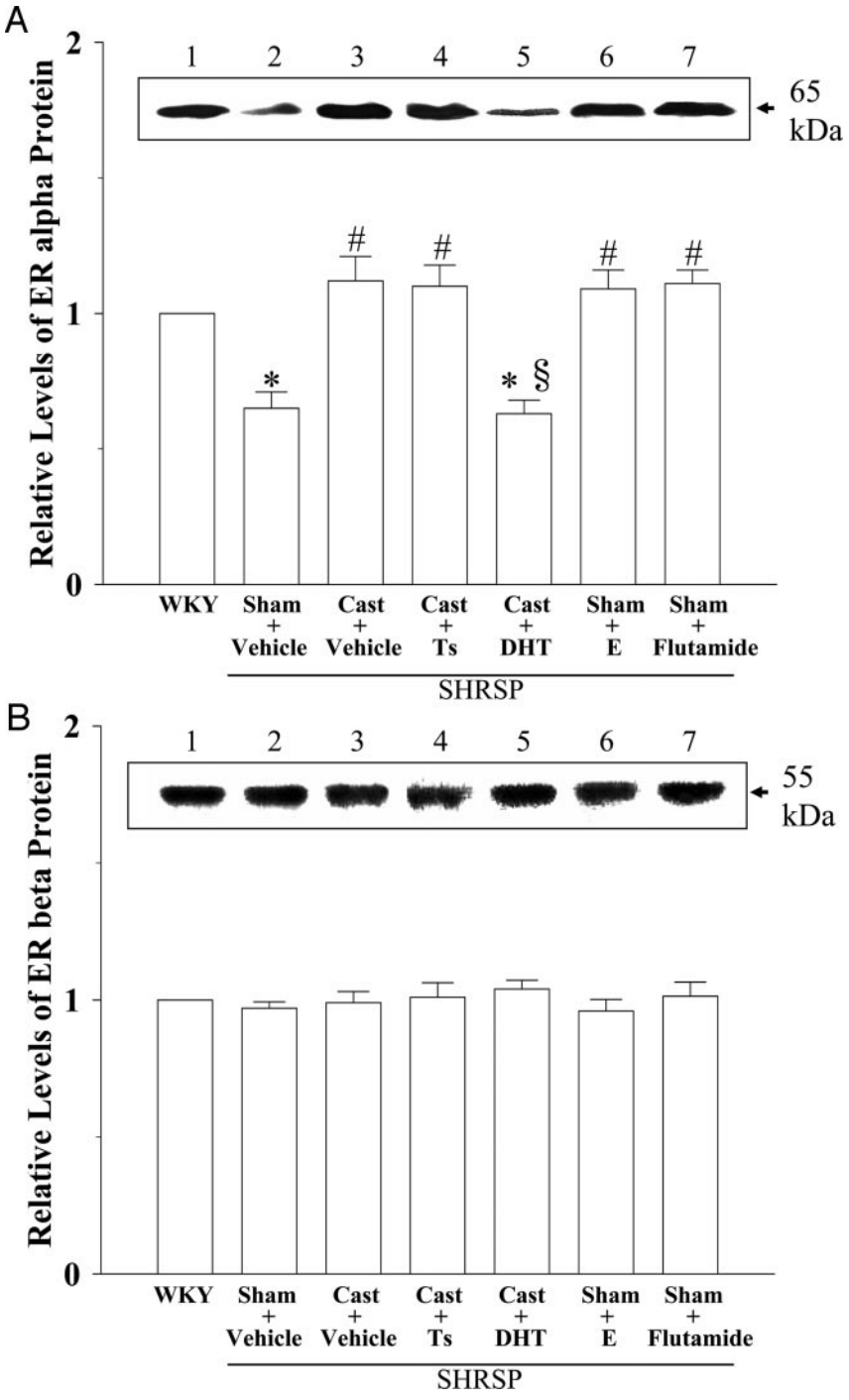

FIG. 5. A and B, Immunoblot analysis for ER*α* (A), and ER*β* (B) in the frontocortical tissues of genetic control WKYs (lane 1), sham-operated SHRSPs (sham+vehicle) (lane 2), castrated SHRSPs [vehicle treated (cast+vehicle) (lane 3); Ts replaced (cast+Ts) (lane 4); DHT replaced (cast+DHT) (lane 5)], sham-operated SHRSPs treated with E (sham+E) (lane 6), and sham-operated SHRSPs treated with flutamide (sham+flutamide) (lane 7). The experiments were conducted by loading equal amounts of proteins in each lane. The *panel of bands*, just above the histogram, shows representative blots of the type of animal and/or treatment, as described above. The intensity of the bands were plotted as histograms, as shown below each panel. In each of the experiments, the band obtained with control WKYs is normalized as 1.0. Data are shown as means ± SD of five separate experiments for ER*α* and of six separate experiments for ER*β*. Statistical analysis was done using one-way ANOVA followed by Scheffé's multicomparison test for basal data obtained from densitometry from each experiment before normalization. *, $P < 0.001$ *vs.* WKY; #, $P < 0.001$ *vs.* sham-operated SHRSP; §, $P < 0.001$ *vs.* castrated SHRSP (vehicle).

pared with age-matched WKYs but counteracted by castration, exogenous estrogens, or AR antagonist flutamide. DHT, but not Ts, reversed the up-regulatory effects of castration on the target molecules. Interestingly, levels of AR were up-regulated in sham and castrated SHRSPs treated with DHT but down-regulated by castration and E or flutamide. Levels of ER*β* remained unchanged. These findings are novel and provide new and important insights that may lead to improved understanding of the pathogenesis of male preponderance and cerebral blood flow abnormalities associated with AD/HD.

Even though volumetric abnormalities in rCBF are common in AD/HD patients (5–11), no study to date has investigated mechanism(s) or factors likely to underlie this phenomenon. The present study revealed marked reductions in levels of an important CNS angiogenic factor, VEGF, its key signaling machinery (VEGF, KDR, Flt-1, pAkt, eNOS) in the frontocortical region of sham-operated SHRSPs. The decrease in levels of active or pAkt, a critical downstream molecule that mediates VEGF-induced angiogenesis and phosphorylates eNOS, indicates a compromise of VEGF signaling in sham-operated SHRSPs. However, Akt in the brain

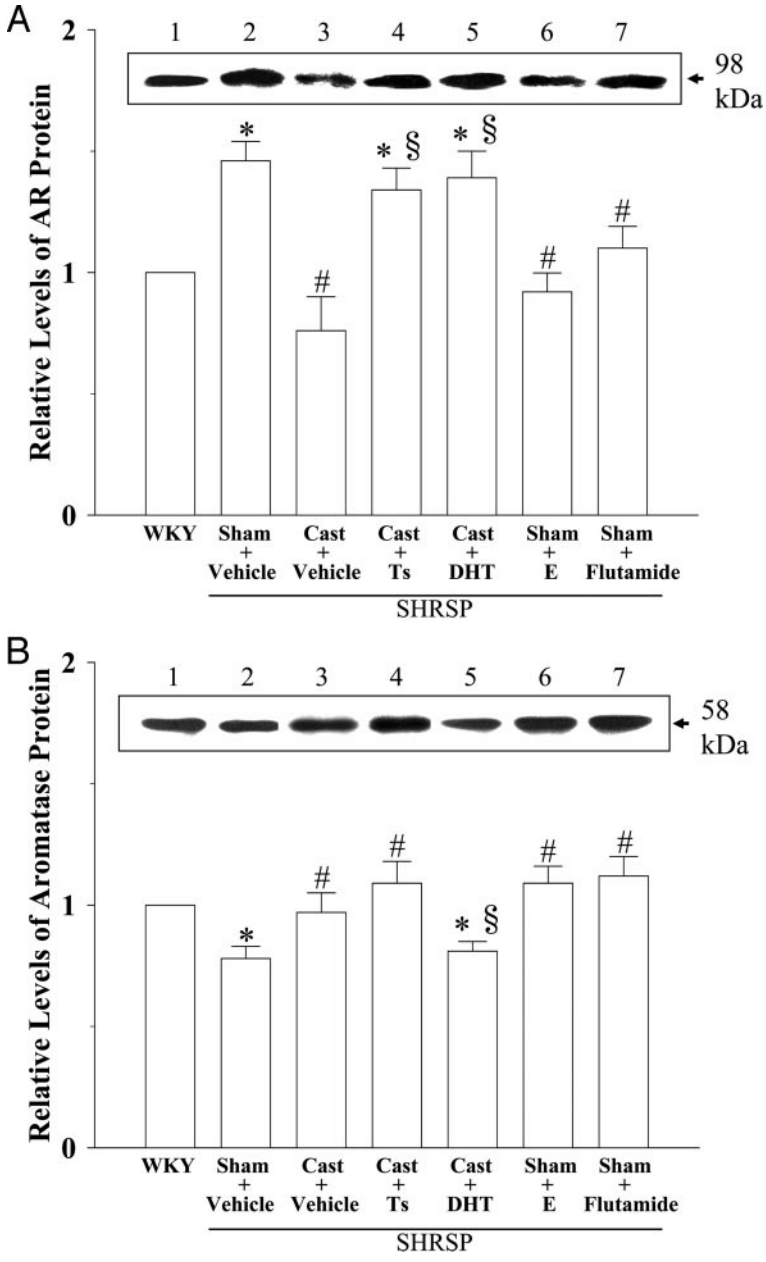

FIG. 6. A and B, Immunoblot analysis for AR (A), and aromatase (B) in the frontocortical tissues of genetic control WKYs (lane 1), sham-operated SHRSPs (sham+vehicle) (lane 2), castrated SHRSPs [vehicle treated (cast+vehicle) (lane 3); Ts replaced (cast+Ts) (lane 4); DHT replaced (cast+DHT) (lane 5)], sham-operated SHRSPs treated with E (sham+E) (lane 6), and sham-operated SHRSPs treated with flutamide (sham+flutamide) (lane 7). The *panel of bands*, just above the histogram, shows representative blots of the type of animal and/or treatment, as described above. The intensity of the bands were plotted as histograms, as shown below each panel. In each of the experiments, the band of control WKYs was normalized as 1.0. Statistical analysis was done for the basal data before normalization using one-way ANOVA followed by Scheffé's multicomparison test. *, $P < 0.001$ *vs.* WKY; #, $P < 0.001$ *vs.* sham-operated SHRSP; §, $P < 0.001$ *vs.* castrated SHRSP (vehicle).

can also be phosphorylated by other factors, other than VEGF, such as estrogen (60). Because cerebral microvessels account for a considerable portion of total resistance to cerebral blood flow, which is coupled to brain metabolism (61), we also investigated capillary density in the frontal cortex of sham-operated SHRSPs. A concomitant decrease in capillary density, as revealed by lectin staining, and previous functional data showing rCBF reduction in juvenile male SHRSPs (62), are consistent with these observations. Moreover, the molecular and morphological changes observed here are consistent with rCBF data in 6-wk-old male WKYs and SHRSPs in parallel experiments conducted in our laboratory: rCBF in WKYs was 33.60 ± 11.09 (ml/min per 100 g tissue, n = 8) and 21.99 ± 7.50 (ml/min per 100 g tissue, n = 8) in SHRSPs.

It is reasonable, based on literature, to state that alterations of VEGF concentration to the degree observed in the present study could prove fatal, particularly if they occur at a critical time during brain development (63, 64). Coincidentally, in the rodents, the critical time when the VEGF-dependent neuronal metabolism peaks runs from postnatal d 5–9 until a time when the metabolic needs of the developing brain tissues are established (63–65). Following this establishment, VEGF production is known to decrease and blood flow normalized. This report is the first to reveal marked reductions in VEGF/Akt/eNOS signaling cascade in an animal model for AD/HD. The precise explanation for the marked reduction in VEGF and its signaling system reported here are not completely clear. However, because reduced rCBF and male preponderance both commonly occur in both SHSRP and AD/HD patients and because both estrogen and Ts promote VEGF produc-

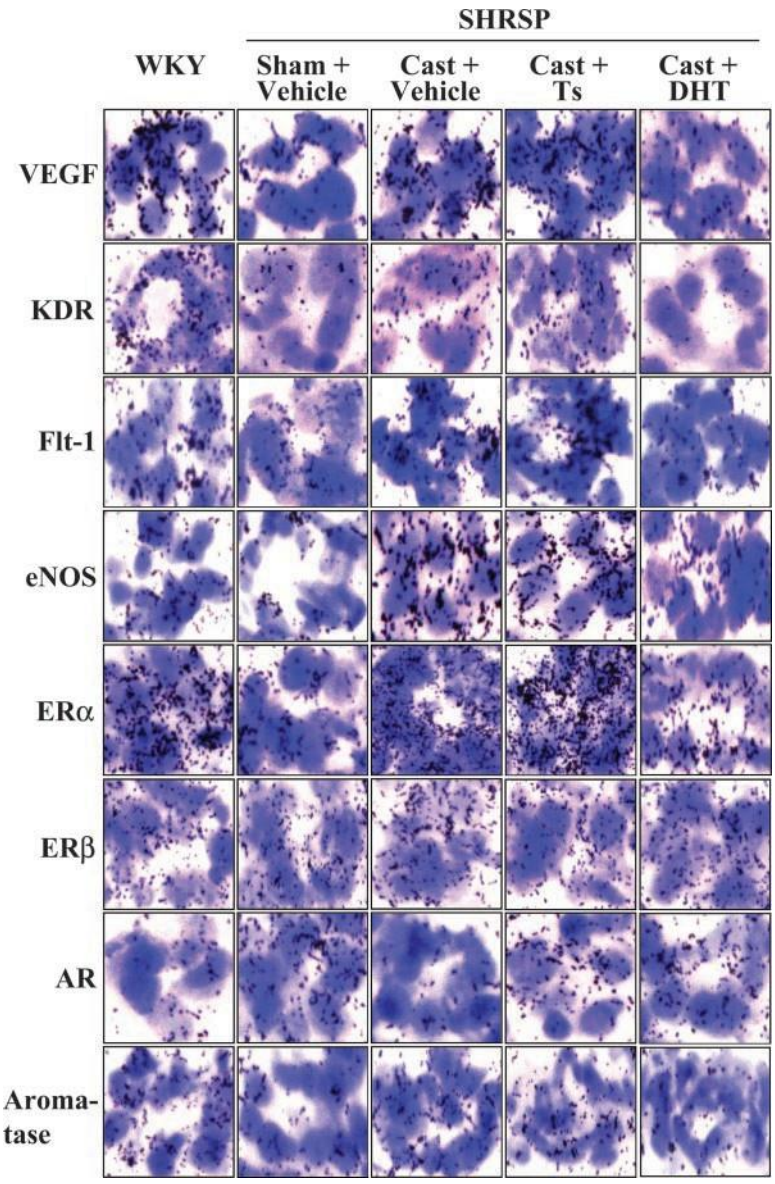

FIG. 7. *In situ* hybridization analysis showing gene expression of VEGF, KDR, Flt-1, eNOS, ER*a*, ER*b*, AR, and aromatase in the coronal section of the frontal cortex from genetic control WKYs, sham-operated SHRSP (sham+vehicle), castrated, vehicle-treated SHRSPs (cast+vehicle), castrated SHRSP replaced with Ts (cast+Ts), and castrated SHRSPs replaced with DHT (cast+DHT). Nuclei of cerebral vessels (internal diameter < 100 μm) stained with hematoxylin appear bluish violet and target mRNAs appear as *black grains*. Magnification, ×400.

tion *in vivo* and *in vitro* and VEGF promoter contains response elements for both hormones, changes in gonadal hormone synthesis or metabolism may likely influence VEGF synthesis and signaling. We know that Ts up-regulates VEGF expression in tissues such as higher vocal center of songbird neostriatum (66) and ventral prostate of castrated rats (38) and estrogen stimulates VEGF synthesis in tissues such as the female reproductive organs (39). Indeed, deletion of Ts effects by castration diminished levels of VEGF expression in the frontal cortex of juvenile male Wistar rats (Jesmin, S., unpublished observation, 2003). On the other hand, in sham-operated juvenile male SHRSPs, levels of VEGF and its associated molecules were significantly down-regulated but up-regulated by castration and exogenous estrogen or AR antagonist flutamide. Most importantly, DHT, but not Ts, attenuated the enhanced levels of VEGF and its angiogenic signaling cascade induced by castration.

Collectively, the present findings appear to point to DHT as a factor that is likely to trigger disruption of VEGF and its associated molecules. This conclusion is further supported by the fact that plasma levels of DHT in juvenile SHRSPs were significantly higher than those of WKYs, and expression of aromatase in frontal cortex was significantly lower than WKYs. Indeed, a recent report showing that DHT blocks E-induced VEGF production (67) and that interference with 5*a*-reduction of Ts attenuates androgen-induced male behaviors (68) are consistent with our conclusion. Alternatively, however, two of the major metabolites downstream of DHT, namely 3*a*-diol and 3*b*-diol, could influence levels of angiogenic molecules (69). Higher levels of 3*a*-diol, which functions as a weak androgen and is readily reconverted to DHT, are likely to favor similar outcomes as DHT outlined above because it is capable of inducing Ts-regulated aggression and acts on ')-aminobutyric acid-A receptor (68–70). 3*b*-Diol, on the other hand, which can also be reconverted to DHT, has estrogenic activity with lower affinities for ER, *i.e.* 10- and

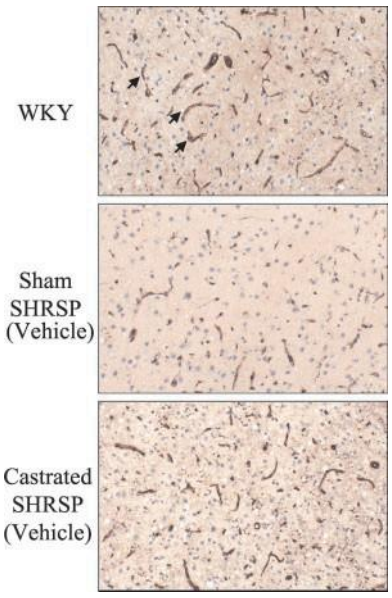

FIG. 8. Evaluations of capillaries in the coronal sections of the frontal cortex from genetic control WKYs, sham-operated SHRSPs (vehicle), and castrated SHRSPs (vehicle). Photomicrographs show capillary endothelial cells immunostained with lectin. *Arrow* indicates capillary in the frontal cortex. Nuclei of the cells in the frontal cortex were stained with hematoxylin. Magnification, X100.

30-fold lower for ER*β* and ER*α*, respectively, compared with that of estradiol (71–74). The estrogenic effects of 3*β*-diol, which under the present experimental conditions tend to attenuate the effects of DHT in SHRSPs, seem unlikely because of its poor affinity for ER (73).

Knowledge of the role of androgen and estrogen systems in the development of male behavior has greatly expanded in the recent past. Whereas Ts plays a key role in the masculinization process of the male brain (31), estrogen ensures a timely shift from the predominantly estrogenic prenatal phase to a predominantly androgenic postnatal phase by up-regulating AR levels. Therefore, it is possible that alterations in receptor levels of either hormones or possibly in the ratio or rate of E/DHT conversion from Ts, as highlighted here, could compromise the E/androgen-regulated processes in brain development. This could include vascular function and, possibly, lead to a predisposition to AD/HD development. Moreover, alterations in E/androgen systems may, in part, help to explain etiology of male preponderance observed in SHRSPs.

Estrogen is believed to play an important function in psychiatric disorders (75), and recent evidence by ER gene deletion studies show that both ER*α* and -*β* are involved in the regulation of different types of male behaviors (76). In the present study, only levels of ER*α*, but not ER*β*, decreased in the frontal cortex of sham-operated SHRSPs, an effect reversed by E, flutamide, castration, or treatment of castrated SHRSPs with Ts. Furthermore, in addition to low ER*α* expression, frontocortical aromatase and circulating E levels were also disrupted in sham-operated SHRSPs, compared with genetic control WKYs. Interestingly, when DHT was given to castrated SHRSPs, it down-regulated the elevated levels of ER*α* induced by castration. These findings are consistent with previous clinical data implicating ER*α* in the pathogenesis of cognitive diseases such as schizophrenia, a bipolar disorder, but most importantly, AD/HD (20). Collectively, the above data indicate that the inhibitory effects of DHT on ER*α* and aromatase expression might be mediated by AR. The present findings correlate with data of previous studies, which localized ER*α* in discrete areas of human brain related to cognition (77), and our most recent work, which revealed a 1:3 ratio of ER*α* and ER*β* levels in the frontal cortex of middle-aged female rat (53). Moreover, ER knockout (ERKO) mice studies have shown a marked reduction in frontal cortex-regulated male aggression behavior in ER*α*KO (78) but, on the contrary, a significant increase in ER*β*KO mice (79). Furthermore, locomotion activity, which is disrupted in AD/HD (hyperactivity), is completely abolished in ER*α*KO but not in ER*β*KO (80). It is worth noting that the molecular data of the present study matched those of the behavioral studies, submitted elsewhere. Arguably, it is too early at this point to link alterations of ER*α* levels to AD/HD. More work is required to elucidate the specific roles of ER*α* and -*β* because levels of ER*β* in the cerebral cortex, hippocampus, and basal forebrain, critical sites for cognition function, are far greater than those of ER*α*. Additionally, more investigations are required to demonstrate the precise nature of the interaction between E and Ts in SHRSPs.

In contrast to SHRSP, when WKYs were castrated, attentional performance tended to worsen, although this was not statistically significant. Castration of SHRSPs reversed the behavioral and attentional abnormalities in SHRSPs, a model of AD/HD (data submitted elsewhere). Moreover, whereas castration of SHRSPs up-regulated VEGF levels in the frontal cortex, it down-regulated levels of VEGF in WKYs by about 15%. This should not be surprising because androgens are known to induce VEGF expression in a variety of tissues (38, 66). These are the striking differences between the two rat strains in both attention performance and VEGF levels after castration, which prompted us launch detailed investigations into the SHRSPs.

The dosage of E used in the present treatments, although effective in improving behavioral abnormalities and frontocortical vascular factor expressions in SHRSP, is, admittedly, on the higher side. It is, therefore, essential that future studies determine the minimum dosage of E, which will restore normal attentional performance and the levels of frontocortical vascular factors in SHRSPs.

In summary, we conclude that alterations in gonadal hormone metabolism during development of frontocortical neurons could alter VEGF angiogenic signaling cascade. This, in turn, may trigger volumetric abnormalities in cerebral blood flow of frontal cortex in SHRSPs and, consequently, compromise the supply of essential nutrients and elements for optimal neuronal activity and brain function. Although the brain development time-line between rodent and man are remarkably consistent (81), it is obviously premature at this point to extrapolate the present data to humans. However, the present animal model and data do lay some foundation for future studies aimed at elucidating mechanisms likely to underlie volumetric abnormalities in frontal cerebral blood flow of AD/HD, an essential step in the effective management of AD/HD.

Acknowledgments

Received April 15, 2004. Accepted May 27, 2004.

Address all correspondence and requests for reprints to: Ichiro Sakuma, M.D., Department of Cardiovascular Medicine, Hokkaido University Graduate School of Medicine, Sapporo 060-8638, Japan. E-mail: sakuichi@seagreen.ocn.ne.jp.

This work was supported in part by a grant-in-aid for scientific research from the Ministry of Education, Science, Sports, and Culture of Japan and Health Sciences Research grants for comprehensive research on aging and health from the Ministry of Health, Welfare, and Labor of Japan.

References

1. **American Psychiatric Association** 1994 Attention-deficit and disruptive behavior disorders. In: Diagnostic and statistical manual of mental disorders, DSM-IV. Washington, DC: American Psychiatric Association; 78–85
2. **Castellanos FX, Giedd JN, Eckburg P, Marsh WL, Vaituzis AC, Kaysen D, Hamburger SD, Rapoport JL** 1994 Quantitative morphology of the caudate nucleus in attention deficit hyperactivity disorder. Am J Psychiatry 151:1791–1796
3. **Taylor E** 1998 Clinical foundations of hyperactivity research. Behav Brain Res 94:11–24
4. **Lahey BB, Applegate B, McBurnett K, Biederman J, Greenhill L, Hynd GW, Barkley RA, Newcorn J, Jensen P, Richters J, Garfinkel B, Kerdyk L, Frick PJ, Ollendick T, Perez D, Hart EL, Waldman I, Shaffer D** 1994 DSM-IV field trials for attention deficit hyperactivity disorder in children and adolescents. Am J Psychiatry 151:1673–1685
5. **Lou HC, Henriksen L, Bruhn P** 1984 Focal cerebral hypoperfusion in children with dysphasia and/or attention deficit disorder. Arch Neurol 41:825–829
6. **Zametkin AJ, Liotta W** 1998 The neurobiology of attention-deficit/hyperactivity disorder. J Clin Psychiatry 59:17–23
7. **Castellanos FX** 1997 Toward a pathophysiology of attention-deficit/hyperactivity disorder. Clin Pediatr (Phila) 36:381–393
8. **Giedd JN, Blumenthal J, Molloy E, Castellanos FX** 2001 Brain imaging of attention deficit/hyperactivity disorder. Ann NY Acad Sci 931:33–49
9. **Gustafsson P, Thernlund G, Ryding E, Rosen I, Cederblad M** 2000 Associations between cerebral blood flow measured by single photon emission computed tomography (SPECT), electroencephalogram (EEG), behaviour symptoms, cognition and neurological soft signs in children with attention-deficit hyperactivity disorder. Acta Paediatr 89:830–835
10. **Kim BN, Lee JS, Shin MS, Cho SC, Lee DS** 2002 Regional cerebral perfusion abnormalities in attention deficit/hyperactivity disorder. Statistical parametric mapping analysis. Eur Arch Psychiatry Clin Neurosci 252:219–225
11. **Spalletta G, Pasini A, Pau F, Guido G, Menghini L, Caltagirone C** 2001 Prefrontal blood flow dysregulation in drug naive ADHD children without structural abnormalities. J Neural Transm 108:1203–1216
12. **Becker JB** 1999 Gender differences and influences of reproductive hormones on dopaminergic function in striatum and nucleus accumbens. Pharmacol Biochem Behav 64:803–812
13. **McEwen BS, Gould E, Orcinik M, Weiland NG, Wooley CS** 1995 Oestrogens and the structural and functional plasticity of neurons: implications for memory, ageing and neurodegenerative processes. In: Goode J, ed. The non-reproductive actions of sex steroids. Ciba Foundation Symposium. London: John Wiley & Sons, Inc.; 191:52–73
14. **McEwen BS, Alves SH** 1999 Estrogen actions in the central nervous system. Endocr Rev 20:279–307
15. **King JA, Barkley RA, Delville Y, Ferris CF** 2000 Early androgen treatment decreases cognitive function and catecholamine innervation in an animal model of ADHD. Behav Brain Res 107:35–43
16. **Comings DE, Chen C, Wu S, Muhleman D** 1999 Association of the androgen receptor gene (AR) with ADHD and conduct disorder. Neuroreport 10:1589–1592
17. **King JA, Kelly TA, Delville Y** 2000 Adult levels of testosterone alter catecholamine innervation in an animal model of attention-deficit hyperactivity disorder. Neuropsychobiology 42:163–168
18. **Comings DE, Gade-Andavolu R, Gonzalez N, Wu S, Muhleman D, Blake H, Chiu F, Wang E, Farwell K, Darakjy S, Baker R, Dietz G, Saucier G, MacMurray JP** 2000 Multivariate analysis of associations of 42 genes in ADHD, ODD and conduct disorder. Clin Genet 58:31–40
19. **Sawada H, Shimohama S** 2000 Neuroprotective effects of estradiol in mesencephalic dopaminergic neurons. Neurosci Biobehav Rev 24:143–147
20. **Feng J, Yan J, Michaud S, Craddock N, Jones IR, Cook Jr EH, Goldman D, Heston LL, Peltonen L, Delisi LE, Sommer SS** 2001 Scanning of estrogen receptor α (ERα) and thyroid hormone receptor α (TRα) genes in patients with psychiatric diseases: four missense mutations identified in ERα gene. Am J Med Genet 105:369–374
21. **Biederman J, Faraone SV** 2002 Current concepts on the neurobiology of attention-deficit/hyperactivity disorder. J Atten Disord 6(Suppl 1):S7–S16
22. **Carlsson ML** 2001 On the role of prefrontal cortex glutamate for the antithetical phenomenology of obsessive compulsive disorder and attention deficit hyperactivity disorder. Prog Neuropsychopharmacol Biol Psychiatry 25:5–26
23. **Prohovnik I, Arnold SE, Smith G, Lucas LR** 1997 Physostigmine reversal of scopolamine-induced hypofrontality. J Cereb Blood Flow Metab 17:220–228
24. **Mack CM, McGivern RF, Hyde LA, Denenberg VH** 1996 Absence of postnatal testosterone fails to demasculinize the male rat's corpus callosum. Brain Res Dev Brain Res 95:252–255
25. **Arnold AP, Breedlove SM** 1985 Organizational and activational effects of sex steroids on brain and behavior: a reanalysis. Horm Behav 19:469–498
26. **Hernandez L, Gonzalez L, Murzi E, Paez X, Gottberg E, Baptista T** 1994 Testosterone modulates mesolimbic dopaminergic activity in male rats. Neurosci Lett 171:172–174
27. **Stewart J, Rajabi H** 1994 Estradiol derived from testosterone in prenatal life affects the development of catecholamine systems in the frontal cortex in the male rat. Brain Res 646:157–160
28. **Dougherty DD, Bonab AA, Spencer TJ, Rauch SL, Madras BK, Fischman AJ** 1999 Dopamine transporter density in patients with attention deficit hyperactivity disorder. Lancet 354:2132–2133
29. **Krause KH, Dresel SH, Krause J, Kung HF, Tatsch K** 2000 Increased striatal dopamine transporter in adult patients with attention deficit hyperactivity disorder: effects of methylphenidate as measured by single photon emission computed tomography. Neurosci Lett 285:107–110
30. **Arnold A, Gorski R** 1984 Gonadal steroid induction of structural sex differences in the central nervous system. Annu Rev Neurosci 7:413–442
31. **MacLusky N, Naftolin F** 1981 Sexual differentiation of the central nervous system. Science 211:1294–1303
32. **Baum MJ, Brand T, Ooms M, Vreeburg JT, Slob AK** 1988 Immediate postnatal rise in whole body androgen content in male rats: correlation with increased testicular content and reduced body clearance of testosterone. Biol Reprod 38:980–986
33. **Pang SF, Tang F** 1984 Sex differences in the serum concentrations of testosterone in mice and hamsters during their critical periods of neural sexual differentiation. J Endocrinol 100:7–11
34. **Kim BN, Lee JS, Cho SC, Lee DS** 2001 Methylphenidate increased regional cerebral blood flow in subjects with attention deficit/hyperactivity disorder. Yonsei Med J 42:19–29
35. **Ueno K, Togashi H, Mori K, Matsumoto M, Ohashi S, Hoshino A, Fujita T, Saito H, Minami M, Yoshioka M** 2002 Behavioural and pharmacological relevance of stroke-prone spontaneously hypertensive rats as an animal model of a developmental disorder. Behav Pharmacol 13:1–13
36. **Ueno K, Togashi H, Matsumoto M, Ohashi S, Saito H, Yoshioka M** 2002 $\alpha4\beta2$ Nicotinic acetylcholine receptor activation ameliorates impairment of spontaneous alternation behavior in stroke-prone spontaneously hypertensive rats, an animal model of attention deficit hyperactivity disorder. J Pharmacol Exp Ther 302:95–100
37. **Agrawal R, Conway GS, Sladkevicius P, Payne NN, Bekir J, Campbell S, Tan SL, Jacobs HS** 1999 Serum vascular endothelial growth factor (VEGF) in the normal menstrual cycle: association with changes in ovarian and uterine Doppler blood flow. Clin Endocrinol (Oxf) 50:101–106
38. **Haggstrom S, Lissbrant IF, Bergh A, Damber JE** 1999 Testosterone induces vascular endothelial growth factor synthesis in the ventral prostate in castrated rats. J Urol 161:1620–1625
39. **Albrecht ED, Pepe GJ** 2003 Steroid hormone regulation of angiogenesis in the primate endometrium. Front Biosci 8:d416–d429
40. **Storment JM, Meyer M, Osol G** 2003 Estrogen augments the vasodilatory effects of vascular endothelial growth factor in the uterine circulation of the rat. Am J Obstet Gynecol 183:449–453
41. **Virgintino D, Errede M, Robertson D, Girolamo F, Masciandaro A, Bertossi M** 2003 VEGF expression is developmentally regulated during human brain angiogenesis. Histochem Cell Biol 119:227–232
42. **Haigh JJ, Morelli PI, Gerhardt H, Haigh K, Tsien J, Damert A, Miquerol L, Muhlner U, Klein R, Ferrara N, Wagner EF, Betsholtz C, Nagy A** 2003 Cortical and retinal defects caused by dosage-dependent reductions in VEGF-A paracrine signaling. Dev Biol 262:225–241
43. **Luthman J, Fredriksson A, Lewander T, Jonsson G, Archer T** 1989 Effects of *d*-amphetamine and methylphenidate on hyperactivity produced by neonatal 6-hydroxydopamine treatment. Psychopharmacology (Berl) 99:550–557
44. **Giros B, Jaber M, Jones SR, Wightman RM, Caron MG** 1996 Hyperlocomotion and indifference to cocaine and amphetamine in mice lacking the dopamine transporter. Nature 379:606–612
45. **Sagvolden T** 2000 Behavioral validation of the spontaneously hypertensive rat (SHR) as an animal model of attention-deficit/hyperactivity disorder (AD/HD). Neurosci Biobehav Rev 24:31–39
46. **Sagvolden T, Berger DF** 1996 An animal model of attention deficit disorders: the female shows more behavioral problems and is more impulsive than the male. Eur Psychologist 1:113–122
47. **Wultz B, Sagvolden T, Moser EI, Moser M-B** 1990 The spontaneously hypertensive rat as an animal model of attention-deficit hyperactivity disorder: effects of methylphenidate on exploratory behavior. Behav Neural Biol 53:88–102
48. **Nakamura K, Shirane M, Koshikawa N** 2001 Site-specific activation of do-

pamine and serotonin transmission by aniracetam in the mesocorticolimbic pathway of rats. Brain Res 897:82–92
49. **Togashi H, Kimura S, Matsumoto M, Yoshioka M, Minami M, Saito H** 1996 Cholinergic changes in the hippocampus of stroke-prone spontaneously hypertensive rats. Stroke 27:520–525
50. **Togashi H, Minami M, Bando Y, Koike Y, Shimamura K, Saito H** 1982 Effects of clonidine and guanfacine on drinking and ambulation in spontaneously hypertensive rats. Pharmacol Biochem Behav 17:519–522
51. **Togashi H, Matsumoto M, Yoshioka M, Hirokami M, Minami M, Saito H** 1994 Neurochemical profiles in cerebrospinal fluid of stroke-prone spontaneously hypertensive rats. Neurosci Lett 166:117–120
52. **Togashi H, Ueno K, Jesmin S, Sakuma I, Matsumoto M, Inoue Y, Yoshioka M,** Effects of gonadectomy and gonadal hormone replacement on short-term memory impairment in an animal model of attention-deficit /hyperactivity disorder. Proc 33rd Annual Meeting of the Society for Neuroscience, New Orleans, Louisiana, 2003 (Abstract 668.4)
53. **Jesmin S, Hattori Y, Sakuma I, Liu MY, Mowa CN, Kitabatake A** 2003 Estrogen deprivation and replacement modulate cerebral capillary density with vascular expression of angiogenic molecules in middle-aged female rats. J Cereb Blood Flow Metab 23:181–189
54. **Jesmin S, Sakuma I, Hattori Y, Kitabatake A** 2002 *In vivo* estrogen manipulations on coronary capillary network and angiogenic molecule expression in middle-aged female rats. Arterioscler Thromb Vasc Biol 22:1591–1597
55. **Jesmin S, Mowa CN, Matsuda N, Salah-Eldin AE, Togashi H, Sakuma I, Hattori Y, Kitabatake A** 2002 Evidence for a potential role of estrogen in the penis: detection of estrogen receptor-*α* and -*β* messenger ribonucleic acid and protein. Endocrinology 143:4764–4774
56. **Jesmin S, Sakuma I, Salah-Eldin A, Nonomura K, Hattori Y, Kitabatake A** 2003 Diminished penile expression of vascular endothelial growth factor and its receptors at the insulin-resistant stage of a type II diabetic rat model: a possible cause for erectile dysfunction in diabetes. J Mol Endocrinol 31:401–418
57. **Jesmin S, Hattori Y, Sakuma I, Mowa CN, Kitabatake A** 2002 Role of ANG II in coronary capillary angiogenesis at the insulin-resistant stage of a NIDDM rat model. Am J Physiol Heart Circ Physiol 283:H1387–H1397
58. **Mowa CN, Iwanaga T** 2001 Expression of estrogen receptor-*α* and -*β* mRNAs in the male reproductive system of the rat as revealed by *in situ* hybridization. J Mol Endocrinol 26:165–174
59. **Lauber ME, Lichtensteiger W** 1994 Pre- and postnatal ontogeny of aromatase cytochrome P450 messenger ribonucleic acid expression in the male rat brain studied by *in situ* hybridization. Endocrinology 135:1661–1668
60. **Znamensky V, Akama KT, McEwen BS, Milner TA** 2003 Estrogen levels regulate the subcellular distribution of phosphorylated Akt in hippocampal CA1 dendrites. J Neurosci 23:2340–2347
61. **Joo F** 1985 The blood-brain barrier *in vitro*: ten years of research on microvessels isolated from the brain. Neurochem Int 7:1–25
62. **Yamori Y, Horie R** 1977 Developmental course of hypertension and regional cerebral blood flow in stroke-prone spontaneously hypertensive rats. Stroke 8:456–461
63. **Ogunshola OO, Stewart WB, Mihalcik V, Solli T, Madri JA, Ment LR** 2000 Neuronal VEGF expression correlates with angiogenesis in postnatal developing rat brain. Brain Res Dev Brain Res 119:139–153
64. **Bar T** 1980 The vascular system of the cerebral cortex. Adv Anat Embryol Cell Biol 59:1–62
65. **Robertson PL, Dubois M, Bowman PD, Goldstein GW** 1985 Angiogenesis in developing rat-brain—an *in vivo* and *in vitro* study. Dev Brain Res 23:219–223
66. **Louissaint Jr A, Rao S, Leventhal C, Goldman SA** 2002 Coordinated interaction of neurogenesis and angiogenesis in the adult songbird brain. Neuron 34:945–960
67. **Kanda N, Watanabe S** 2002 17*β*-Estradiol enhances vascular endothelial growth factor production and dihydrotestosterone antagonizes the enhancement via the regulation of adenylate cyclase in differentiated THP-1 cells. J Invest Dermatol 118:519–529
68. **Frye CA, Rhodes ME, Walf A, Harney JP** 2002 Testosterone enhances aggression of wild-type mice but not those deficient in type I 5*α*-reductase. Brain Res 948:165–170
69. **Weihua Z, Andersson S, Cheng G, Simpson ER, Warner M, Gustafsson JA** 2003 Update on estrogen signaling. FEBS Lett 546:17–24
70. **Labrie F, Luu-The V, Labrie C, Simard J** 2001 DHEA and its transformation into androgens and estrogens in peripheral target tissues: intracrinology. Front Neuroendocrinol 22:185–212
71. **Hackenberg R, Turgetto I, Filmer A, Schulz KD** 1993 Estrogen and androgen receptor mediated stimulation and inhibition of proliferation by androst-5-ene-3*β*, 17*β*-diol in human mammary cancer cells. J Steroid Biochem Mol Biol 46:597–603
72. **Ho SM, Ofner P** 1986 Prostatic cytosol binding of 5*α*-androstane-3*β*, 17*β*-diol and estradiol-17*β*. Steroids 47:21–34
73. **Kuiper GG, Carlsson B, Grandien K, Enmark E, Haggblad J, Nilsson S, Gustafsson JA** 1997 Comparison of the ligand binding specificity and transcript tissue distribution of estrogen receptors *α* and *β*. Endocrinology 138: 863–870
74. **Verjan HL, Eik-Nes KB** 1977 Comparison of effects of C19 (androstene or androstane) steroids on serum gonadotrophin concentrations and on accessory reproductive organ weights in gonadectomized, adult male rats. Acta Endocrinol 84:829–841
75. **McEwen B** 2002 Estrogen actions throughout the brain. Recent Prog Horm Res 57:357–384
76. **Ogawa S, Lubahn DB, Korach KS, Pfaff DW** 1997 Behavioral effects of estrogen receptor gene disruption in male mice. Proc Natl Acad Sci USA 94:1476–1481
77. **Osterlund MK, Keller E, Hurd YL** 2000 The human forebrain has discrete estrogen receptor *α* messenger RNA expression: high levels in the amygdaloid complex. Neuroscience 95:333–342
78. **Ogawa S, Washburn TF, Taylor J, Lubahn DB, Korach KS, Pfaff DW** 1998 Modifications of testosterone-dependent behaviors by estrogen receptor-*α* gene disruption in male mice. Endocrinology 139:5058–5069
79. **Nomura M, Durbak L, Chan J, Smithies O, Gustafsson JA, Korach KS, Pfaff DW, Ogawa S** 2002 Genotype/age interactions on aggressive behavior in gonadally intact estrogen receptor *β* knockout (*β*ERKO) male mice. Horm Behav 41:288–296
80. **Ogawa S, Chan J, Gustafsson JA, Korach KS, Pfaff DW** 2003 Estrogen increases locomotor activity in mice through estrogen receptor *α*: specificity for the type of activity. Endocrinology 144:230–239
81. **Clancy B, Darlington RB, Finlay BL** 2001 Translating developmental time across mammalian species. Neuroscience 105:7–17